The Waves of a Walker – An Experimental Study of the Mechanism Behind the Movement of Walkers

Goni Yoeli and Nir Livne

A droplet of liquid may bounce indefinitely on a vertically vibrating bath of the same liquid. If the vibration is close enough to the bath's Faraday instability threshold, the droplet can become a 'walker', and begin to propagate in a constant velocity. It has been shown that this system has quantum-like characteristics, while the governing physical properties are clearly measurable. This system is thought to be an experimental playground for concepts in the pilot-wave interpretation of quantum mechanics.

In this paper, we investigate the wavefield created by a walker using FS-SS transparent surface measurement technique. We show that the waves that allow a walker to move are subharmonic sinusoidal standing waves, that decay in time and space, and that these waves were aroused by the previous bounces of the walker. We then suggest that these waves are linear, and simulate the propagation of the droplet according to our findings. A generalization of our research, which could be done using the same technique, may provide explanation to many of the observed phenomena.

Introduction

When a droplet falls onto a surface of the same fluid, surface tension tends to minimize the entire surface area, and eventually leads to the merger of the droplet and the bulk - as expected based on our intuition. Even so, the coalescence is not instantaneous – it takes time since the air film at the interface between the two needs to drain (Couder 2005). It was first documented by Walker that a vertically vibrating surface may allow a droplet to bounce indefinitely. It is doing so by supplying the droplet with enough vertical momentum, quickly enough, when the two come into contact (Walker 1978).

In 2006, Couder showed that under certain conditions, bouncing droplets begin to move horizontally and become *walkers*, as the system's acceleration approaches values where the Faraday instability is triggered (Couder 2006a). Above this threshold, Faraday waves spontaneously appear throughout the entire vessel. Theses waves are parametrically-forced waves, who's wavelength obeys the dispersion relation typical to gravity-capillary waves[1].

As we shall see later, the transition to walkers happens due to interaction between the moving droplet and the surface wavefield (WF) it's exciting when hitting the liquid surface.

Couder extended his research and found many quantum-like phenomena such as single and double slit diffractions patterns (Fort & Couder 2006), tunneling (Eddi et al. 2009), quantized orbits (Fort, Eddi, & Couder 2010), etc. This is a rare record of a classical (macro scaled) particle exhibiting behavior once thought to be unique to the micro scaled quantum physics. In contrast of a Copenhagen quantum particle, the measurements in these cases do not change the walker's physical properties, and the system is clearly deterministic. A better analogue to this system is the deterministic (and realistic) pilot-wave theory which was initially proposed by De Broglie. This theory was abandoned by most of the physics community but never truly refuted (though proven non-local).

As a deterministic system, given enough information about its initial state, we would like to be able to describe its evolution in time. Many steps are to be made in order to construct a full theory of this time development. Among these steps is understanding of the exact coupling between a droplet and its WF. We focus on investigating the WF aroused by single impact in regions where walkers emerge, with eyes to a more precise and general study of this inspiring subject.

Experimental Setup

A circular vessel made of acrylic glass with a diameter of $20cm$ was attached to a shaker (figure 1). The container was filled up to 3mm in height with silicone oil with viscosity of $\mu = 10\ mPa\ s$, surface tension of $\sigma = 0.02\frac{N}{m}$ and mass density of $\rho = 930\frac{kg}{m^3}$ (Aldrich 378321). The walls of the container were coated with silicone seal and shaped to 45° in order minimize boundary effects caused by meniscus waves. The entire setup was carefully set perpendicular to the floor. The shaker was set to vibrate in sinusoidal form ($\ddot{x} = \gamma g\cos(2\pi f t)$),

[1] The dispersion relation is $\omega^2 = gk + \frac{\sigma}{\rho}k^3$, where ω is half the forcing frequency, σ is the surface tension, and ρ is the liquid's mass density.

where $f = 80Hz$, g is the gravitational acceleration and γ is dimensionless amplitude).

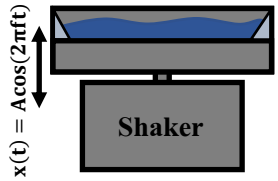

Figure 1. The experimental setup. A circular vessel was attached to a shaker, which was set to vibrate in sinusoidal waveform. The vessel's walls were coated with silicone seal to minimize boundary effects.

Results

Bouncing droplets of various sizes (with radius in the order of 0.5mm) became walkers and began moving horizontally when forcing the of the system reached $\gamma = 4.11 \pm 0.02$, while the Faraday instability threshold was experimentally found at $\gamma = 4.23 \pm 0.05$. These became our lower and upper bounds in the following measurements. In this region of forcing amplitudes, the droplets transit from bouncing harmonically (bouncing at the same frequency as the shaker) to sub-harmonically (bouncing at half the forcing frequency). Our first observation showed that without any external interference, walkers seemed to be moving at constant velocity (with velocities in the order of $5\frac{mm}{sec}$), and in seemingly straight lines towards at a random direction (appendix A). This stable movement clearly cannot be caused by noise (like air flows), and the direction of propagation can even be chosen. The transition of the system at $\gamma \approx 4.11$ also rules out standard conservation of momentum of the drop as a complete explanation. Since no other cause is apparent, a natural assumption would be that the droplets propagate because they interact with waves on the surface of the vibrating liquid - in a way which grants them a constant boost of velocity. We could now infer that as a droplet lands on a surface with a non-zero gradient, momentum passes to it, both vertically and horizontally (figure 2). Before a walker is introduced to the system, there are no waves present. We can therefore conclude that walkers are the source of the WF that guides their horizontal movement.

In order to understand the nature of these waves, we simulated a single impact of a droplet by creating a disturbance on the vibrating surface using a toothpick (similar to a delta-function disturbance). We measured the propagation speed of the traveling wave emitted to be[2] $17.2 \pm 1.2\ \frac{cm}{sec}$ (appendix B). A simple calculation of the distance that the traveling wave has passed between two consecutive bounces of the droplet, reveals that it has traveled about 4mm, while the walker has traveled only about 0.1mm. We could now deduce that walkers cannot interact with the traveling waves that they produce, since the traveling waves are long gone by the time the droplets bounces again.

Baring these facts in mind, we then proceeded to measure the surface height ($h(x,y,t)$) more accurately, thinking that there should be more to the WF than the traveling waves. We used an image correlation technique called FS-SS (Moisy, Rabaud & Salsac 2009). FS-SS is a technique based on PIV (particle image velocimetry) algorithm and linearization of Snell's law. In simple terms, a geometrical pattern is placed at the bottom of the liquid container. An image of the pattern is taken from above while the surface of the liquid is still. Once waves are introduced, the image of the pattern seems to be deformed compared to the reference image, in accordance to Snell's law. These deformations can be measured by taking a second image and comparing the local displacement field between the images using a PIV algorithm (appendix C). We executed the algorithm using PIVLab add-in for MATLAB (Thielicke & Stamhuis 2014). Now, assuming the camera-surface distance is much larger than the region of interest (small paraxial angles), and that the deformations of the liquid surface are small, the surface gradient is linearly proportional to the displacement field (Moisy et al. 2009). The last step required to reconstruct the surface height $h(x,y,t)$ is to integrate the gradient field, which was done by d_2 norm minimization using Intgrad2 MATLAB function (John D'Errico 2006).

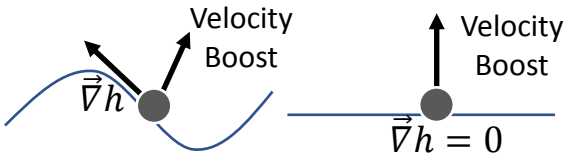

Figure 2. A diagram showing how momentum could pass to the droplet not only vertically (due to the parametric oscillations), but also horizontally when the gradient field is non-zero ($\vec{\nabla}h \neq 0$).

[2]The theoretical phase velocity that suits the dispersion relation under the conditions in this study is $18.1\ \frac{cm}{sec}$.

Using these methods, we observed that following a single disturbance to the liquid's surface, a circular traveling wave is triggered. As it is moving outwards, a localized standing wave is left behind (figure 3). This standing wave has a well-defined wavelength of $\lambda = 4.5 \pm 0.2mm$, which is a near perfect fit to the theoretical (and measured) Faraday wavelength (corresponding to this liquid and forcing frequency) predicted by the dispersion relation[3]. We suggest that as the traveling wave spreads away from the point of impact, it excites many different wavelengths, but only the ones that are connected to the parametric forcing of the oscillating vessel are sustained, while the rest decay quickly. The mechanism of the formation of these standing waves should be addressed in future research.

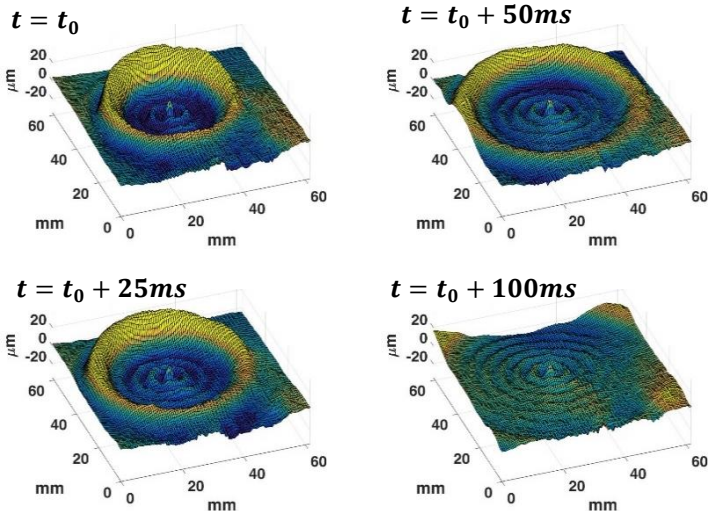

Figure 3. The time evolution of the wavefield after a single impact caused by a toothpick. The top-left image was captured at $t_0 \approx 150ms$ following the impact. The system was driven at 80Hz and amplitude $\gamma = 4.12 \pm 0.02$. Images were taken at 1,000 fps.

Our next goal was to try to make a simple (linear) model that could explain why these droplets are moving. We set out to model the standing WF created by a walker, and to create a computer simulation according to our findings, which would retrieve results that are similar to the measured results.

Before we proceed to simulating the interaction of a droplet with its WF, we have to characterize the standing WF itself. First, we should measure what it looks like in space and time, i.e. $\psi(\vec{r}, t)$. Next, if we want to make a linear model, we will have to assure that these waves are linear, which means that we can superimpose many impacts in a linear fashion.

To make things simpler, we assumed superposition at first. If exists, it suggests that we could learn about the standing WF created by a walker by studying the WF of a single impact. We returned to the measurement presented in figure 3 and measured the WF's spatial waveform (figure 4A). We found that the best fit for our measurements is of the spatial form of $\psi(\vec{r}) = Ae^{-\frac{r}{\rho}}\cos(2\pi\frac{r}{\lambda})$, where A is the amplitude at $r = 0$, λ is the measured wavelength, and ρ is the typical decay length, which was measured to be $20 \pm 5mm$ (appendix D) under the mentioned conditions. It was also observed that ρ is related to the proximity to the Faraday instability threshold – the closer the system is to the threshold, the larger ρ is, but further research is required to quantify this effect.

Our next task was to measure the time evolution of these standing waves. This could be divided into two parts. First, there's a sinusoidal oscillation of the entire WF at half the forcing frequency, as to be expected in many parametrically forced systems. The second time dependence of the WF is its decay over time – since the system is below the Faraday instability threshold, the waves caused by each impact will eventually die out. To measure its decay over time, the amplitude of the standing WF was measured at a few different maxima, once every period of oscillation. The best fit we found to the amplitude decay over time was an exponential decay (figure 4B), which means that we found the temporal dependence of the standing waves to be of the form $T(t) = e^{-\frac{t}{\tau}} \cdot \cos(\pi f \cdot t)$, where τ is the typical decay time, which was measured to be $\tau = 0.19 \pm 0.01\ s$. It should be noted that as with ρ (the typical decay distance) we observed that τ is related to the Faraday instability threshold – the closer we are to the threshold, the longer it takes for the waves to decay over time (τ becomes larger). For this reason, it should be kept in mind that our results refer only to this specific setup, and different values are to be excepted when using different liquids or forcing.
It may be instructive to search for a connection between ρ and τ in future studies, but to this date, no relation was found.

[3] $\lambda_{theory} = 4.58mm$ according to the dispersion relation.

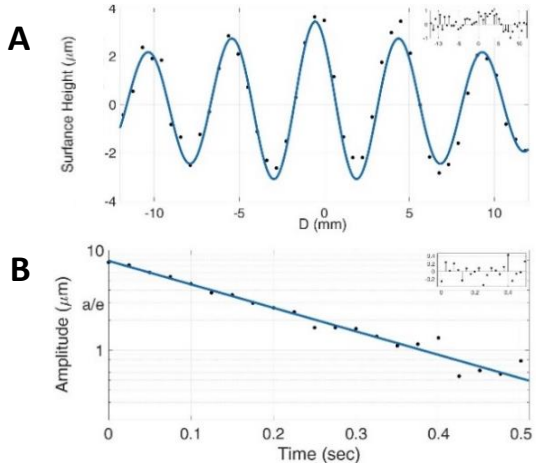

Figure 4. The spatial and temporal waveform of the standing waves. (A) The standing waves are clearly symmetric to rotations around the point of impact, so only a cross-section is needed to describe the waves. The best fit for the measurements is a function of the type $\psi(\vec{r}) = Ae^{\frac{-r}{\rho}}\cos(2\pi\frac{r}{\lambda})$, where $\rho = 20 \pm 5mm$ is the typical decay distance, and λ is the measured wavelength. (B) Temporal decay of the standing waves. The amplitude of the standing waves was measured once every cycle (40Hz). The data shows an exponential decay over time, with typical decay time of $\tau = 0.19 \pm 0.01\ s$. The measurement was made at $\gamma = 4.12 \pm 0.02$.

The above measurements provide us with a phenomenological description of the standing WF created by a single impact on the liquid surface, which altogether reads:

$$\psi(\vec{r},t) = Ae^{-(\frac{t}{\tau}+\frac{r}{\rho})}\cos\left(2\pi\frac{r}{\lambda}\right)\cos(\pi f t)$$

We would like to note that this WF is the one governing the system only after the traveling wave has passed, but as we have shown before, it is the one relevant to the propagation of walkers. We believe our results provide a good approximation to this WF, but as mentioned earlier, a theoretical description is still needed.

The last step before trying to model the interaction between a droplet and its associated WF would be to make sure that these standing waves are linear. To check this assumption, we created a disturbance using two toothpicks that were attached to each other (few cm apart), and then attempted see if the results match what would be expected from the superposition of two single disturbances (figure 5). We have found that for our purposes (small amplitudes and beneath the Faraday instability threshold), these waves *seem* linear. We believe that with more knowledge about the waveform of the standing waves created we could show an even better fit. The reasoning behind our belief is that when we attempted to replicate the results measured after a double-toothpick disturbance, by superimposing two *measurements* of a single-toothpick disturbance, we have found even more similarities between the WFs (the data is not shown because currently the measurements are too noisy at small amplitudes to stack them).

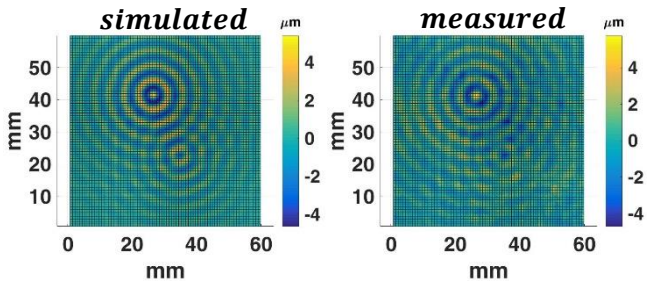

Figure 5. A comparison between the measured wavefield of a double-toothpick impact (right), and the superposition of two distinct standing waves as modeled in the previous sections (left). The measured wavefield is the field present at the surface after the traveling wave has left the ROI. Measurements were made at 80Hz, while the acceleration amplitude was $\gamma = 4.14 \pm 0.02$.

With this information in hand, we now attempted to simulate the propagation of walkers. The droplet receives momentum from the oscillating liquid bath. Since the oscillations are vertical, the droplet can only gain horizontal momentum if it gains momentum in a way that is proportional to the gradient of the surface WF, that is $\Delta P_{horizontal} = f(\vec{\nabla}h)$.

After studying the mean speed of a walker, we saw that it travels about $\frac{1}{40}$ th of the wavelength of the standing waves between bounces. If the droplet's previous point of impact is the center of the standing wave, we can deduce that the droplet lands on a gradient field which is *nearly* zero (based on our previous measurements of the WF). In addition, simple calculations can show that the vertical boost in momentum is about 20 times the boost in the horizontal direction (Appendix F). These could suggest that it is enough to consider the linear approximation of $f(\vec{\nabla}h)$, that is $\Delta P_{horizontal} = \alpha\vec{\nabla}h$, where α could depended on many parameters (such as droplet size, oil characteristics, forcing amplitude, etc.). It was suggested before that this relation is linear (Couder 2011), and our newly gained knowledge could support that. When a droplet touches the surface of the liquid, it must lose a lot of its momentum gained at previous bounce because of energy considerations (the droplet's speed does not diverge but remains fairly constant). This could be explained by the transfer of energy to heat due to friction, or by the transfer of energy to the traveling wave that is emitted.

We now constructed a simulation of the movement of a walker by the following algorithm:

1) A droplet begins with some arbitrary speed (which could be gained by any spontaneous breaking of symmetry)
2) As the droplet hits the surface of the liquid, it creates a standing wave with spatial and temporal dependencies of the form measured before. This wave is linearly added to the existing WF.
3) When the droplet hits the surface, it loses most of its momentum (due to friction losses or others), and gains momentum by bouncing on a non-zero gradient field, in accordance to the following equation: $v(t_i) = \beta v(t_{i-1}) - \alpha\vec{\nabla}h$, where t_i is the time of the i[th] cycle since the beginning of the simulation.
4) The droplet moves in constant horizontal velocity until it hits the surface again.
5) The simulation will jump back to step 2.

We executed the algorithm in MATLAB (Appendix E). It was seen that only if $\beta \ll 1$, the speed walkers could be kept reasonable compared to the propagation speeds measured. After choosing the amplitude of the standing wave (which could depend on the droplet size and forcing amplitude for example), only a narrow range of values of α allowed for the droplet to become a walker. This could explain why in reality, once the liquid is chosen and the conditions are set, only a narrow range of droplet sizes become walkers.

The results of our simulations closely resemble the WF created by a propagating droplet (figure 6). The same interference patterns can be seen in both the measured WF, and in the computer simulation. Moreover, as mentioned before, the simulation replicated the movement of walkers as a movement at constant mean velocity.

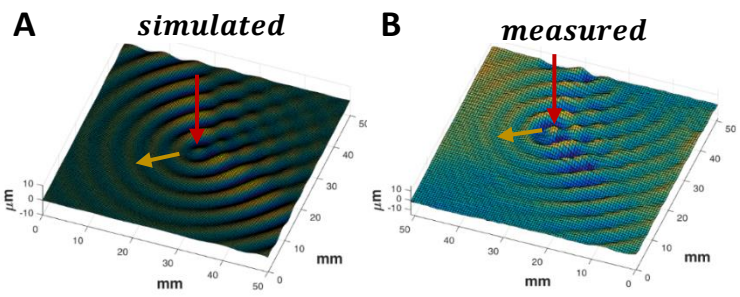

Figure 6. A comparison between the measured wavefield created by a walker (right) and a simulation of the wavefield (left). Red arrows indicate the location of the previous bounce of the droplet, and yellow arrows indicate its direction of propagation. Measurements were made at forcing amplitude of $\gamma = 4.11 \pm 0.02$

Conclusion

In summary, we have shown that a walker is in fact a droplet which is constantly interacting with its own emitted standing wavefield. We proposed a model for the spatial and temporal dependencies of these standing waves, and showed (to some extent) that these waves are linear. We then continued to test our models by using a computer simulation, and replicated both the movement in constant mean velocity, and the interference patterns that are typical of a physical walker.

The standing wavefield is clearly non-localized compared to the droplet size and the traveling speed of a walker. We therefore propose that many of the phenomena in which the system is thought to have complex quantum-like behavior could be the result of this intricate coupling between a particle (a droplet) and its guiding wave (its own created wavefield). We believe that the inspiring phenomena seen by others could be investigated using the results of this study, and techniques we have developed.

Acknowledgments

We would like to thank Prof. Ronen Rapaport and Prof. Eran Sharon for their guidance and support.

References

Couder, Y., Fort, E., Gautier, C. H., & Boudaoud, A. (2005). From bouncing to floating: noncoalescence of drops on a fluid bath. *Physical review letters*, *94*(17), 177801.

Couder, Y., & Fort, E. (2006). Single-particle diffraction and interference at a macroscopic scale. *Physical review letters*, *97*(15), 154101.

D'Errico J, "Inverse (integrated) gradient" for Matlab. http://www.mathworks.com/matlabcentral/. File 9734.

Eddi, A., Fort, E., Moisy, F., & Couder, Y. (2009). Unpredictable tunneling of a classical wave-particle association. *Physical review letters*, *102*(24), 240401.

Eddi, A., Sultan, E., Moukhtar, J., Fort, E., Rossi, M., & Couder, Y. (2011). Information stored in Faraday waves: the origin of a path memory. *Journal of Fluid Mechanics*, *674*, 433-463.

Fort, E., Eddi, A., Boudaoud, A., Moukhtar, J., & Couder, Y. (2010). Path-memory induced quantization of classical orbits. *Proceedings of the National Academy of Sciences*, *107*(41), 17515-17520.

Moisy, F., Rabaud, M., & Salsac, K. (2009). A synthetic Schlieren method for the measurement of the topography of a liquid interface. *Experiments in Fluids*, *46*(6), 1021.

Nikolai Chernov, "Circle Fit (Pratt Method)" for Matlab. http://www.mathworks.com/matlabcentral/. File 22643.

Protière, S., Boudaoud, A., & Couder, Y. (2006). Particle–wave association on a fluid interface. *Journal of Fluid Mechanics*, *554*, 85-108.

Thielicke, W., & Stamhuis, E. (2014). PIVlab–towards user-friendly, affordable and accurate digital particle image velocimetry in MATLAB. *Journal of Open Research Software*, *2*(1).

Tinevez, J. Y., Perry, N., Schindelin, J., Hoopes, G. M., Reynolds, G. D., Laplantine, E., ... & Eliceiri, K. W. (2017). TrackMate: An open and extensible platform for single-particle tracking. *Methods*, *115*, 80-90.

Walker, J. (1978). J. Walker, Sci. Am. 238, No. 6, 123 (1978). *Sci. Am.*, *238*, 123.

Appendix A – the Path of Walkers

The oil container was vibrated vertically at 80Hz, as usual. The amplitude of oscillations was adjusted to allow walkers to exist. A spotlight was held at 45° to the entire bath. Since the surface deformations are minor, and the camera is placed well above the region of interest, the droplets were seen as bright spots on a dark background (droplets are round while the surface is flat compared to them, figure A1a). Pictures were now taken in a high-speed camera once between consecutive bounces, at the same time in each period. After calibrating the pixels into real distances, and preforming image processing such that only pixels bright enough will remain visible (these steps were done in ImageJ, an open-source image processing software), we used a plugin called TrackMate (Tinevez, Perry and Schindelin 2016) to track the location of a droplet along its path in each video (figure A1b).

We now analyzed both the mean speed of propagation of the droplet, and the tilt angle of the droplet's path - that is, how 'straight' is its path. The mean velocities measured were $3-7\frac{mm}{sec}$ (figure A2a), which seemed to depend on the system's acceleration and the droplets' size. The relative tilt angle (θ) was measured by predicting the direction of propagation of a walker along the straight line connecting its' last two bounces, and comparing that to the direction of the actual third bounce. The mean relative θ was nearly zero, while in some measurements it had a slight tilt to one side (figure A2b).

It was observed that abnormal values of propagation velocity and relative θ were due to technical errors in the tracking algorithm.

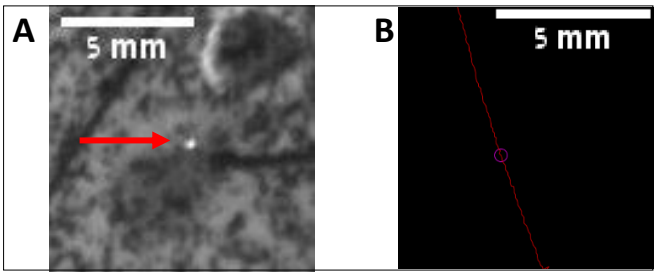

Figure A1. Measuring the path of walkers. (A) A spotlight was held at 45° to the bath, allowing mostly the reflection of the droplet to reach the camera, which made the droplets shine compared to their background. (B) The location of the droplet was recorded in every frame using TrackMate add-in for ImageJ. Images were taken at 160fps (4 times the bouncing frequency)

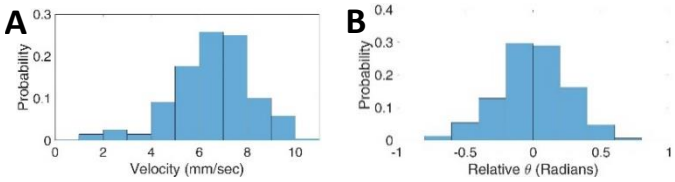

Figure A2. Characteristic histogram of a walker's velocity and path. (A) The mean speed of a walker was measured between each bounce. (B) The angle of rotation of each bounce was compared to the interpolation of the previous two bounces to a straight line. This was our way to quantify how 'straight' is the path of walkers. Both histograms are based on 300 bounces. It was seen that values abnormally different from the mean value are caused by mistakes in the tracking algorithm, as the droplet's movement is made by tiny steps, which could very large compared to our errors.

Appendix B – Velocity of the Traveling Waves

After the surface height $(h(x,y,t))$ was reconstructed (Appendix C), we could measure the velocity of traveling waves in our system. A single disturbance was applied to the liquid surface using a toothpick. A traveling wave of a circular form appear around the point of impact (figure B1). We measured the radius of this growing circle by fitting a circle to the mid-height of the wave (figure B2a). This was done by implementing an algorithm named 'CircleFitByPartt' and calculating the increase of circle diameter over time (figure B2b). A linear increase in radius was measured, which indicates a constant velocity of propagation.

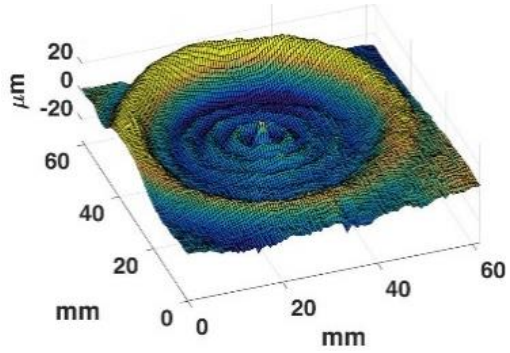

Figure B1. A Traveling wave of circular form was created after disturbing the liquid surface using a toothpick. Images were taken at 1,000 fps.

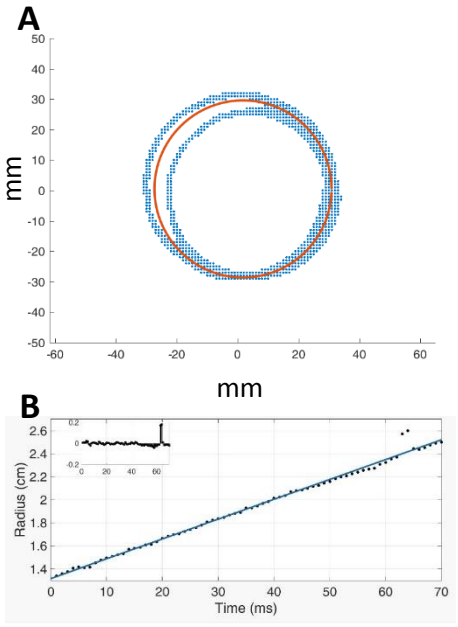

Figure B2. Measuring the radius of the circular traveling wave. (A) A circle was fitted to the mid-height of the traveling wave. (B) Measuring the radius of the traveling wave increase of time can allow us to measure the speed of propagation. A linear increase in radius was measured.

Appendix C – Liquid Surface Reconstruction

In order to reconstruct the surface of the liquid of interest, it was necessary to perform a few steps. First, we would have to record a reference image when there are no waves at the surface, and a second image after an interruption is introduced. Then, we would have to analyze these images to find the difference between them. The last step would be to connect these deformations to the wavefield.

For our first step, which used a high-speed camera that can record images at rates of over 10,000 fps at pixel resolution of 1024x1024. The camera was mounted 170 cm above the oil container and was set perpendicular to it. It is of great importance to keep the camera as tall as possible for step 3. Beneath the lair of silicon oil, we placed a pattern of randomly placed dots of different sizes. As the waves deformed the surface of the oil, a distortion of the random dot was recorded by the camera, in accordance to Snell's law (figure C1).

The next step was to measure the distortion of the random dot pattern. We used an algorithm based on PIV (particle images velocimetry) using an add-in software for MATLAB called PIVLab (Thielicke and Stamhuis 2014). This algorithm is based on the analysis of the difference between a refence image and a second one. The basics of the algorithm are the following:

- Both images are divided into parts. For each sub-image, the algorithm finds the most probable displacement, which would minimize the differences between the reference image and its pair using statistical means (cross-correlation).
- Each sub-image is then divided into smaller sub-images. Using the field of movement found in the previous step, the algorithm refines the displacement field.
- These steps are repeated until reaching the minimal sub-image size, which is determined by the user.

The algorithm can find the displacement field in sub-pixel resolution, given that the right pattern is chosen. We used a pattern made of randomly placed dots, who's sizes are generally related to the interrogation area (sub-images) sizes. This pattern was put through a gaussian filter, which means that the intensity of the dots varies roughly as a gaussian from the center out. The algorithm fits a gaussian to these dots, allowing sub-pixel localization of the displacement field (figure C2).
It is very common for the camera to move between the reference measurement and the deformed-surface-measurement, since even the slightest disturbance to the camera (caused even by its own cooling fan) can have large-scale effects when the camera is mounted this far from the region of interest. For this reason, it was required that before heading to the next step, we subtracted the linear displacement (mean displacement) from the entire displacement field.

The last step in reconstructing the surface height $h(x, y)$ is to connect the displacement field found in the previous step to the gradient of the surface height. It was shown that assuming the camera-surface distance is much larger than the region of

interest (small paraxial angles), and small deformations of the liquid surface, the surface gradient is linearly proportional to the displacement field (Moisy et al. 2009) as follows: $\vec{\nabla}h = -\frac{\delta\vec{r}}{h^*}$, where $\delta\vec{r}$ is the displacement field measured, and h^* is a constant which can be determined by the camera-surface distance, the liquid height, and the refraction index of the liquid. The last step required to reconstruct the surface height $h(x,y)$ is to integrate the gradient field, which was done by d_2 norm minimization using Intgrad2 MATLAB function (John D'Errico 2006).

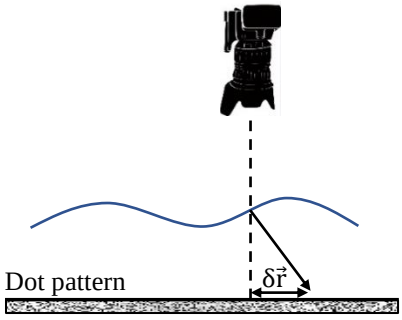

Figure C1. A distortion of the random dot pattern. As waves appear at the surface of the liquid, light-rays reaching each one of the camera pixels will have a slightly different origin compared to the reference image (according to Snell's law), and the image will appear to be distorted.

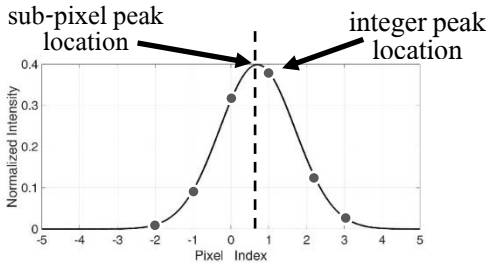

Figure C2. Sub-pixel estimation of the displacement field. The dot-pattern beneath the liquid was put through a gaussian filter – each dot had maximum darkness in its middle and decayed to white in a gaussian form. The PIVLab algorithm could now estimate the gaussian's maximum and retrieve sub-pixel resolution.

Appendix D – Measuring the Standing Waves

The standing waves described are clearly symmetric to rotation around the point of impact (figure 2). It is therefore possible to measure only a cross-section of the wavefield in order to find its spatial dependence.

To measure the spatial waveform, we had to overcome a lot of noise. This noise comes as a local deformation of the surface and was found to be caused by improper lighting in the measurements. To compensate for these noises, we sliced each measured WF at 12 different angles, and averaged over them. Next, we used a MATLAB function to clear any linear trends from the data (the built-in function detrend). We now found which function fits our data best using MATLAB's cftool. These steps were repeated on several different measure WF's (of the same disturbance). When measuring the amplitude of the waves (for the decay over time for example), we used the findpeaks built-in function in MATLAB. It should be mentioned that measuring the spatial dependence of the waves was very technically demanding, and it is plausible that there's a better (but similar) fit for it than the one we suggest.

Appendix E – Simulation of a Walker

The simulation was made according to the algorithm proposed in the article. The main challenge when preforming the simulation is the need to work in many different length-scales, as the drop bounces about 0.1mm in each period, and the wavelength was measured to be about 50 times that size. This could require too much computational power. To solve this problem, we used a grid of medium density – each pixel was about $dx = 0.1mm$ in width. This density only allowed the steps of a walker to be in integer multiplier of dx, which is not good enough. To solve this, we used the interp2 built-in function in MATLAB, which uses cubic interpolation of the digitized field. This allows the estimation of sub-pixel values, and we could now replicate the physical results.

Appendix F – Momentum Boost

The system is forced in a sinusoidal form at 80Hz. Therefore, the acceleration of the system in physical units is $\ddot{x}(t) = A(2\pi f)^2\cos(2\pi f t)$. We can calculate the displacement amplitude, A and find that $A \approx 0.15mm$. By making calculations using the droplet's bouncing period ($\frac{1}{40}$ of a second) we can find that it will reach more than 5 times that height. Assuming the minimal jump height (assuming the system's oscillations are irrelevant to this height), we can find the initial velocity of a walker in the vertical direction to be $v_o = \frac{gt}{2} \approx 100\frac{mm}{sec}$, which is about 20 times the mean horizontal speed of a walker, and is believed to be constant if we neglect air friction.